ChemPubSoc Europe

DOI: 10.1002/chem.201303929

CHEMISTRY
A European Journal
Full Paper

Foldamers

Tuning the Guest-Binding Ability of a Helically Folded Capsule by In Situ Modification of the Aromatic Oligoamide Backbone

Guillaume Lautrette,[a] Christophe Aube,[b] Yann Ferrand,[a] Muriel Pipelier,[b] Virginie Blot,[b] Christine Thobie,[b] Brice Kauffmann,[c] Didier Dubreuil,*[b] and Ivan Huc*[a]

Abstract: Starting from a previously described aromatic oligoamide helically folded capsule that binds tartaric acid with high affinity and diastereoselectivity, we demonstrate the feasibility of the direct in situ modification of the helix backbone, which results in a conformational change that reduces its affinity for guests by two orders of magnitude. Specifically, ring contraction of the central pyridazine unit into a pyrrole in the full helical sequence was investigated by using electrochemical and chemical processes. The sequence containing the pyrrole was synthesized independently in a convergent manner to ascertain its structure. The conformation of the pyrrolic folded capsule was elucidated in the solid state by X-ray crystallography and in solution by using ^{1}H and ^{13}C NMR spectroscopy. Solution studies revealed an unanticipated solvent-dependent equilibrium between the *anti–anti* and *syn–syn* conformations of the pyrrole ring with respect to its two adjacent pyridine units. Titrations of the pyrrole-containing sequence monitored by ^{1}H NMR spectroscopy confirmed the expected drop in affinity for tartaric acid and malic acid that arises from the conformation change in the backbone that follows the replacement of the pyridazine by a pyrrole. The reduction of the pyridazine to a pyrrole was characterized by cyclic voltammetry both on the entire sequence and on a shorter precursor. The lower cathodic potential of the precursor made its preparative-scale electroreduction possible. Direct in situ modification of the pyridazine within the entire capsule sequence was achieved chemically by using zinc in acetic acid.

Introduction

Some helical synthetic foldamers possess a cavity large enough to accommodate guest molecules and constitute a new and efficient approach for the design of synthetic receptors.[1] The self- (or guest induced-) organization of these helical receptors by folding is reminiscent of biological receptors based on the folded conformations of proteins or nucleic acids. In the past decade, different designs of synthetic helical receptors have been described. The simplest consists of open-ended helices that allow rapid guest capture and release.[2] Open-ended receptors have also been designed to bind to dumbbell-shaped guests, which then require a major conformational change in the host to form the host–guest complex by an unfolding–refolding process.[3] An original design consists of closed-shell helically folded capsules comprised of monomers that give a large diameter to impart a cavity in the center of the sequence and of monomers that give a small diameter with no cavity at all at both ends of the sequence, which thus play the role of end-caps.[4] Such capsules have also been made from double-helical structures.[5] In a helical molecular capsule, guest capture and release may occur through a local conformational change in the backbone, with one unit acting as a hinge that opens a temporary window to allow the guest to go through.[6] These capsule designs completely surround the guest and thus offer opportunities to tailor high guest affinity and selectivity.

In principle, complete guest surrounding by a foldamer may also make it possible to control guest capture and release through conformational changes in the backbone induced by external stimuli, as reported for other systems.[7] It is a general property of foldamers to be able to undergo major conformational changes, an extreme case being complete unfolding, from which major changes in properties might be expected to result. Indeed, there have been some examples of folding and

[a] *Dr. G. Lautrette, Dr. Y. Ferrand, Dr. I. Huc*
Université de Bordeaux, CBMN, UMR 5248
Institut Européen de Chimie Biologie
2 rue Escarpit 33607 Pessac (France)
and
CNRS, CBMN, UMR5248 (France)
E-mail: i.huc@iecb.u-bordeaux.fr

[b] *Dr. C. Aube, Dr. M. Pipelier, Dr. V. Blot, Dr. C. Thobie, Prof. D. Dubreuil*
Université de Nantes, CEISAM, UMR6230
Faculté des Sciences et des Techniques, 2 rue de la Houssinière
BP 92208, 44322 Nantes Cedex 3 (France)
and
CNRS, CEISAM, UMR6230 (France)
E-mail: didier.dubreuil@univ-nantes.fr

[c] *Dr. B. Kauffmann*
Université de Bordeaux, UMS3033
Institut Européen de Chimie et Biologie (IECB)
2 rue Escarpit, 33600 Pessac (France)
and
CNRS, IECB, UMS3033 (France)
and
INSERM, IECB, UMS3033 (France)

Supporting information for this article is available on the WWW under http://dx.doi.org/10.1002/chem.201303929.

unfolding of helical oligomers triggered by external stimuli, such as light,[8] metal/ion coordination,[2b,9] or protonation.[10] However, these controlled conformational changes have rarely been coupled to the capture or release of guest molecules.[11] Herein, we demonstrate the feasibility of the direct in situ modification of the backbone of an aromatic oligoamide helical capsule, which results in a conformational change that reduces its affinity towards guest molecules by two orders of magnitude.

Results and Discussion

Design and synthesis

During the last decade, our group has started a systematic investigation aimed at creating new, artificial, rational codes between the primary one-dimensional sequences of aromatic amino acid monomers, their secondary and tertiary three-dimensional folded structures, and their molecular recognition properties.[4] In previous studies, we have shown that receptor **1** was able to complex D/L-tartaric acid with high affinity in organic solvents, with high diastereoselectivity and high selectivity with respect to other carboxylic acid guests (Scheme 1).[4c] In the oligomeric sequence of receptor **1**, the quinoline trimers

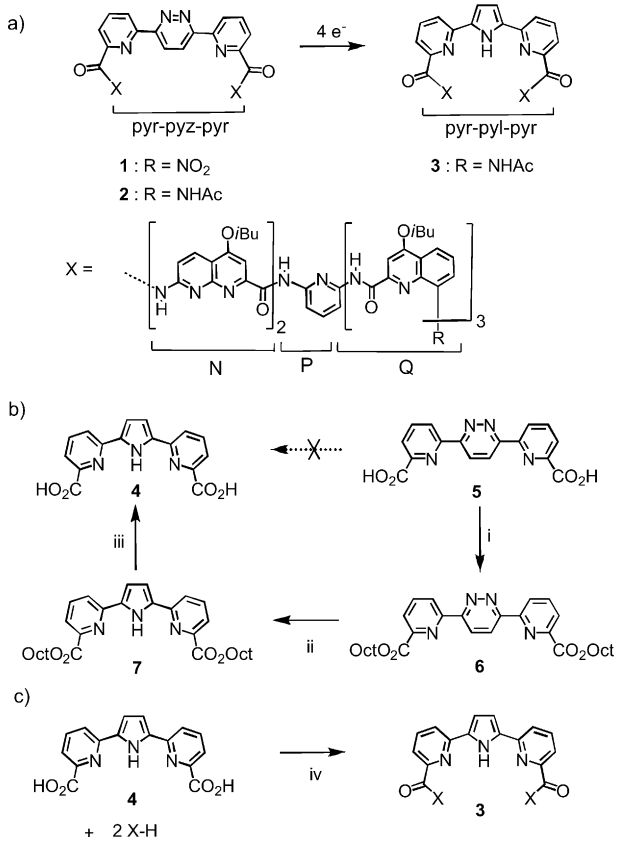

Scheme 1. a) Structure of capsules **1**, **2**, and **3** and abbreviations used for their subunits; b) Synthetic strategy for the preparation of pyr-pyl-pyr diacid **4**: i) $SOCl_2$ then octanol, Et_3N, CH_2Cl_2; ii) controlled-potential electrolysis, $+4e^-$ and $+4H^+$; iii) KOH, MeOH, H_2O; c) Synthesis of capsule **3**: iv) PyBOP, DIPEA, $CHCl_3$.

($\mathbf{Q}_3$) at each extremity form a helix segment with a narrow diameter and act as caps able to close the cavity, whereas the other larger units of the sequence (pyridines (P), naphthyridines (N) and the central pyridyl-pyridazine-pyridyl (pyr-pyz-pyr) segment) serve to create an inner cavity large enough to accommodate a tartaric acid molecule as a guest. In particular, naphthyridines constitute critical elements in the design because of their ability to hydrogen bond to the carboxyl and the hydroxyl functions of the guest.

Previously, we have shown that 3,6-di(pyrid-2-yl)pyridazine segments (pyr-pyz-pyr), as found in the center of sequence **1**, may undergo ring contraction into the corresponding 2,5-di(-pyrid-2-yl)pyrrole through either chemical or electrochemical reductions (Scheme 1 a).[12] To further this concept, we have extended the process to more complex alternating tripyridyl-dipyridazine sequences to form the corresponding tripyridyl-dipyrrole analogues.[13] We also found that, in the solid state, alternating pyridyl-pyrrole-pyridyl linkages (pyr-pyl-pyr) adopted a *syn–syn* conformation stabilized by bifurcated hydrogen bonds between the N*H*-pyrrole and the adjacent endocyclic pyridine nitrogen atoms. Based on this prior knowledge, we speculated that the ring contraction of the central six-membered pyridazine of **1** into a five-membered pyrrole would result in a major change in the curvature of the helix backbone and, consequently, in a loss of affinity for tartaric acid, eventually followed by its release. To test this hypothesis, we first produced capsule **2**, a variant of **1** with terminal acetamido groups instead of nitro groups. Unlike nitro groups, acetamides were expected not to interfere with the electroreduction process of the pyridazine ring, which involves four electrons. Indeed, sequence **3** can be produced by the direct ring contraction of the pyridazine of capsule **2** (see below). Nevertheless, to ascertain its structure, it was independently prepared from its diacid pyrrolic precursor **4** (Scheme 1 b and c).

The preparation of pyr-pyl-pyr diacid **4** was first attempted by ring contraction of the 6,6′-(pyridazin-3,6-diyl)-bis-2-pyridylcarboxylic acid **5** (Scheme 1 b). Unfortunately, the preparative electrolysis of pyr-pyz-pyr diacid **5** failed due to its poor solubility in the solvent mixture used for the electroreduction (THF/acetic buffer/CH_3CN). The introduction of an *n*-octyl ester as a solubilizing group compatible with the electroreduction conditions was carried out by using a diacid chloride and an excess of octanol to give the desired octyl 6,6′-(pyridazin-3,6-diyl)-bis-2-pyridinecarboxylate **6** in 88% yield. As expected, the cyclic voltammogram of dioctyl ester **6** displayed two well-defined irreversible cathodic peaks at −1.09 and −1.43 V versus SCE and a last wave at a more cathodic potential (Figure 1 a). This profile is consistent with the electroreduction mechanism established for the ring contraction of 2,5-dipyridyl-substituted pyridazines into the corresponding pyrroles.[12a,13] However, the larger second reduction wave at $E_{pcII} = -1.43$ V versus SCE, which corresponds to the rearrangement of the dihydropyridazine intermediate into pyrrole, also conceals the reduction peak potential of the ester groups. This observation explains why controlled-potential electrolysis failed to produce corresponding pyrrole derivative **7** in a satisfying manner when run at a mercury pool cathode in a two-compartment cell with

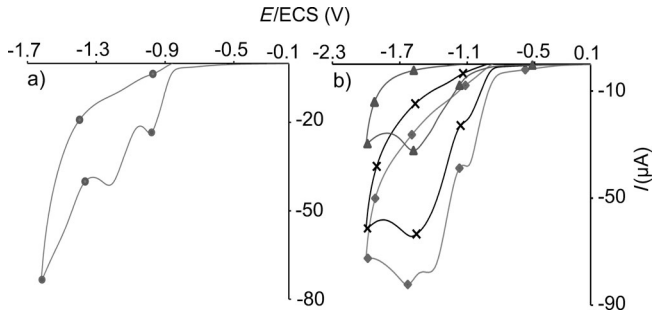

Figure 1. a) Cyclic voltammogram of **6** (1 mM) at a glassy carbon electrode in THF/acetic buffer (pH 4.6)/acetonitrile (5:4:1 v/v/v) at a scan rate of 0.1 Vs^{-1} (●). b) Cyclic voltammogram of **6** (4 mM) at a glassy carbon electrode in THF/acetic buffer (pH 4.6)/acetonitrile (5:4:1 v/v/v) at a scan rate of 0.1 Vs^{-1} before electrolysis (◆), after consumption of 2 e^- (×) and after consumption of 5.2 e^- (▲).

a glass frit, at $E_w = -1.45$ V versus SCE in THF/acetate buffer/CH_3CN (5:4:1 v/v/v). After purification, the pyrrole derivative was isolated in 28% yield along with the formation of alcohol side products. The preparative electroreduction was stopped after consumption of almost five electrons, but the conversion of the starting pyridazine was incomplete. After addition of more than the required four electrons, no evolution of the cyclic voltammetry profile was observed (Figure 1b, ▲). Alternatively, monitoring the electrolysis at the first peak ($E_w = -1.15$ V vs. SCE), which favors a dismutation process,[12a] improves the yield of pyrrole **7** to 51% (four electrons consumed) and all of the remaining starting pyridazine can be recovered.

Saponification of diester **7** was achieved by using KOH in aqueous methanol to give diacid **4** in 85% yield. The assembly of **3** was then undertaken. The first step involved the reduction over Pd/C of the nitro group of the previously described O_2N-**Q_3PN_2**-Boc hexamer,[5c,14] and a subsequent acetylation of the amine product by using acetic anhydride (93% overall yield). The resulting oligomer AcHN-**Q_3PN_2**-Boc was treated with trifluoroacetic acid for Boc cleavage (quantitative) and the resulting amine was coupled to the two acid functions of **4** to give expected capsule **3** in 44% overall yield.

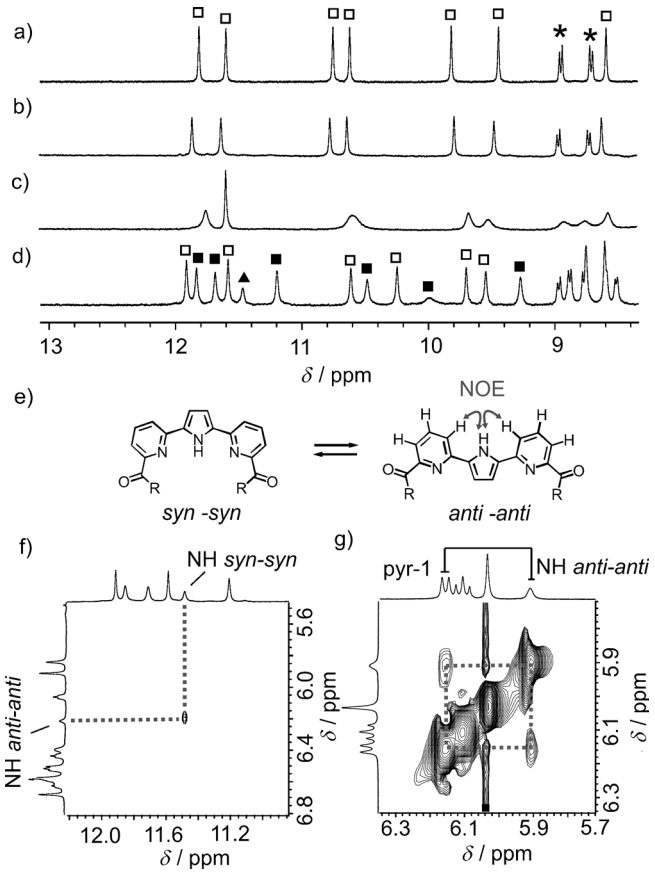

Figure 2. Part of the ^{1}H NMR spectra (400 MHz) of **3** (2 mM) in a) $CDCl_3$ at 298 K, b) $CDCl_3$ at 263 K, c) CD_2Cl_2 at 298 K, and d) CD_2Cl_2 at 263 K. Signals of the *anti–anti* conformation and of the *syn–syn* conformation are marked with □ and ■, respectively; ▲ denotes the resonance of the *syn–syn* N*H* of pyrrole; * indicates some aromatic resonances. e) Scheme representing the equilibrium between the *syn–syn* and *anti–anti* conformations for the pyr-pyl-pyr segment. f) Part of the 2D ROESY NMR spectrum (700 MHz, 263 K) of **3** in CD_2Cl_2, which shows an exchange crosspeak between the signals of the pyrrolic N*H* in *syn–syn* ($\delta = 11.5$ ppm) and *anti–anti* ($\delta = 6.2$ ppm) conformations. g) Part of the 2D NOESY NMR spectrum (700 MHz, 298 K) of **3** in $CDCl_3$, showing strong dipolar couplings between the N*H* of the pyrrole moiety and the protons in position five of the two neighboring pyridines, which indicates a preference for the *anti–anti* conformation.

Solvent-dependent conformational changes

As mentioned above, preliminary studies on the structure of pyr-pyl-pyr-pyl-pyr derivatives hinted at a preferred *syn–syn* conformation of the pyr-pyl-pyr motif in aromatic oligoamide sequences. In comparison with pyridazine capsule **2**, incorporation of a pyrrole five-membered ring should result in a higher curvature, which implies a reduction in the cavity size for helix **3** (see below). The ^{1}H NMR spectrum of **3** at 298 K in $CDCl_3$ showed a single set of sharp peaks, which suggests the existence of a well-defined conformation in solution (Figure 2a). In contrast, a similar measurement performed in CD_2Cl_2 showed a set of broader signals that could correspond to resonances close to coalescence at this temperature (i.e., two or more distinct species in fast exchange, Figure 2c). Indeed, ^{1}H NMR spectra recorded at 263 K revealed again a single set of peaks in $CDCl_3$ (Figure 2b), whereas two sets of well-resolved signals were observed in CD_2Cl_2 (Figure 2d). This behavior contrasts with that of capsules **1** and **2**, which both exist as a single helically folded entity. The existence of two species in the case of helix **3** may thus reasonably be attributed to the pyrrole moiety, presumably due to an exchange between the *syn–syn* and *anti–anti* conformations of the central pyr-pyl-pyr segment in CD_2Cl_2.

Intrigued by this phenomenon, we sought more structural information and 2D NMR spectroscopic analyses were initiated to elucidate the exact nature of the conformational change. A full structural assignment of capsule **3** in $CDCl_3$ by using COSY, HSQC, HMBC, and NOESY experiments allowed us to identify precisely the chemical shift values of protons belonging to the pyrrole moiety (amine and β positions). In $CDCl_3$, intramolecular dipolar couplings between the pyrrolic N*H* at $\delta = 5.9$ ppm and the proton of the neighboring pyridine ($\delta = 6.15$ ppm)

positioned *para* to the amide (Figure 2g) revealed that the pyrrole adopts an unanticipated *anti–anti* configuration when placed in the middle of an aromatic oligoamide sequence. This pyrrole orientation implies that the β-pyrrolic protons point towards the cavity of the capsule, whereas the angle between the carbonyl of pyr-pyl-pyr results in a slightly lower curvature than the one observed for capsule **2**. A ROESY study in CD_2Cl_2 at 263 K allowed us to establish that the pyrrolic N*H* of the *anti–anti* pyr-pyl-pyr at $\delta = 6.2$ ppm is in exchange with a signal at $\delta = 11.5$ ppm (Figure 2f). This latter low-field resonance is typical of a pyr-pyl-pyr sequence in a *syn–syn* conformation due to hydrogen bonding between the N*H* of the pyrrole and the endocyclic nitrogen of the neighboring pyridine. Therefore, in CD_2Cl_2, both *anti–anti* and *syn–syn* conformers coexist. It is unclear why the conformational behavior of the pyr-pyl-pyr segment differs so much in CD_2Cl_2 and $CDCl_3$. A possible explanation may come from the size of solvent molecules and their ability to solvate the inner side of the different conformers of the capsule. Alternatively, differences in the water content of the two solvents may also influence the *anti–anti*/*syn–syn* equilibrium. A full investigation of the solvent-dependent conformational behavior was not undertaken in the context of this study.

X-ray-quality crystals were obtained from the slow diffusion of *n*-hexane into a solution of the capsule **3** in chloroform at room temperature. Crystallographic analysis revealed a perfectly folded capsule with two caps composed of a quinoline trimer at each extremity and a large hollow in the center (Figure 3d and e). The conformation of the pyr-pyl-pyr segment confirmed to be *anti–anti*, as observed in solution in the crystallization solvent (Figure 2f). With this conformation of the central segment, the overall cavity of **3** is slightly longer than that of **1**. For example, the separation between the two carboxamide N*H*s was found to be 8.48 Å in pyr-pyl-pyr in **3** versus 8.15 Å in pyr-pyz-pyr in **1** (Figure 3c and f). A calculation of the internal volume of the cavities of capsules **1** and **3** by using the SURFNET v.1.4 software[15] showed that both cavities have a similar size (≈120 Å^3). However, a major difference resides in the shape of the available space due to the fact that the β-pyrrolic protons protrude largely in the hollow of the helix of **3**, which interferes with the position at which tartaric acid is bound in receptor **1**.

For comparison, we modeled the conformation of capsule **3** with a *syn–syn* central pyr-pyl-pyr segment to give a higher helix curvature (Figure 3g–i). Higher curvature resulted in an increased overall helix length and in a contraction of the cavity to form two compartments with a volume of 73 Å^3 each (Figure 3g). The experimentally observed prevalence of the *anti–anti* over the *syn–syn* conformation in solution and in the solid state was not anticipated and is not consistent with the behavior of pyr-pyl-pyr segments isolated from the context of a longer helically folded oligomer. A comparison of *syn–syn*-**3** and *anti–anti*-**3** structures shows a much more extensive intramolecular π–π overlap in the latter; the *syn–syn* conformation features a kink in its center that causes neighboring naphthyridines to protrude out of the reach of subsequent units for π–π stacking (Figure 3i). It is thus possible that *anti–anti*-**3** is stabilized by intramolecular π–π stacking to the detriment of its *syn–syn* conformation in a sort of induced-fit process.

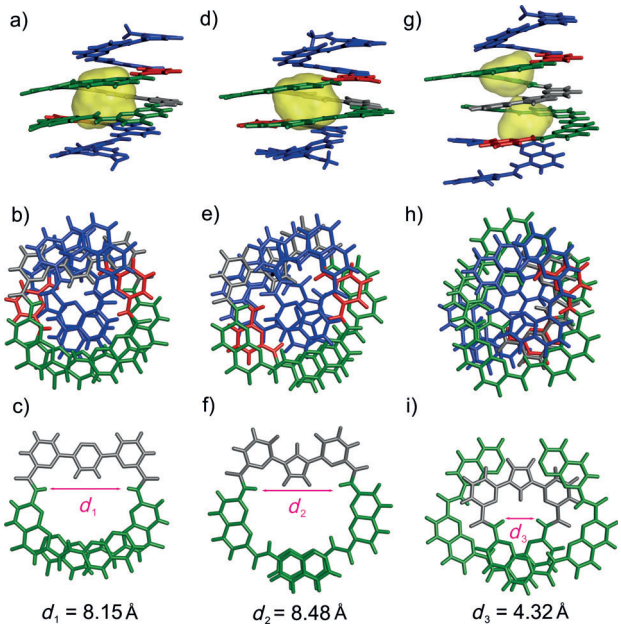

Figure 3. Stick representations of the solid-state structure of the *M*-helix of **1** (Q_3PN_2-pyr-pyz-pyr-N_2PQ_3): a) the side view, b) the top view, and c) a slice of the capsule that shows the N_2-pyr-pyz-pyr-N_2 segment from above.[5c] Stick representations of the solid-state structure of the *M*-helix of **3** (Q_3PN_2-pyr-pyl-pyr-N_2PQ_3 with an *anti–anti* conformation of the pyrrole): d) the side view, e) the top view, and f) a slice of the capsule that shows the N_2-pyr-pyl-pyr-N_2 segment from above. Stick representation of the structure of the *M*-helix of **3** (Q_3PN_2-pyr-pyl-pyr-N_2PQ_3 with a *syn-syn* conformation of the pyrrole) as obtained by molecular modeling (MMFFs force field) by using Maestro v.6.5: g) the side view; h) the top view, and i) a slice of the capsule that shows the N_2-pyr-pyl-pyr-N_2 segment from above. Volumes of cavities are shown as transparent yellow isosurfaces. Isobutoxy groups and solvent molecules are not shown for clarity.

Host–guest chemistry

The effect of the replacement of pyridazine by a pyrrole on the guest recognition of the capsule was first assessed by titrating capsule **3** with D/L-tartaric acid in $CDCl_3$ with 1% [D_6]DMSO to dissolve the guest in the stock solution. Upon increasing the guest concentration, the initial set of signals that correspond to free capsule **3** was progressively replaced by a new set that can be attributed to a **3**⊃D/L-tartaric acid complex (Figure 4). The exchange between the empty capsule and the **3**⊃D/L-tartaric acid complex was found to be slow on the NMR spectroscopy timescale, which confirms that the guest encapsulation requires a partial unfolding of the helix. The existence of a single set of sharp signals for **3**⊃D/L-tartaric acid is indicative of a complete diastereoselectivity (*de* > 99%), whereas the circular dichroism spectra confirm that the D enantiomer of tartaric acid was encapsulated in the *P*-helix of **3** (positive band at $\lambda = 360$ nm, Figure S7 in the Supporting Information) as observed for helix **1**. The addition of one equivalent of guest did not result in the saturation of receptor **3**, as observed in the case of **1**, which proves that the affinity of **3** for tartaric acid is significantly lower than that of **1** (Figure 4a and

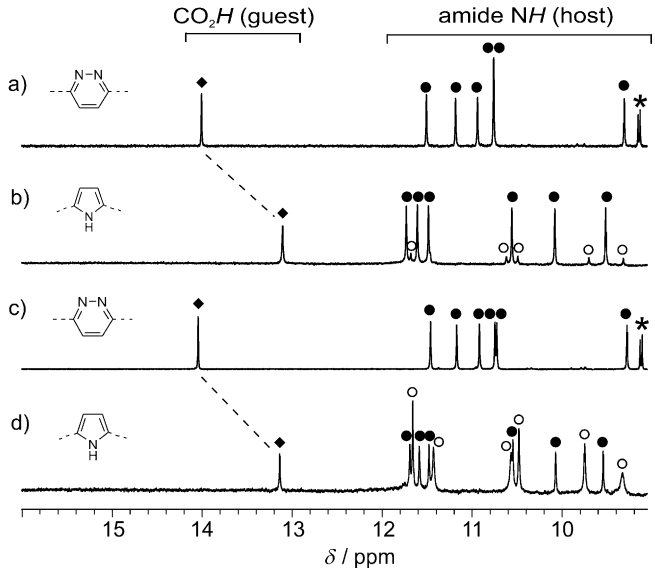

Figure 4. Part of the ^{1}H NMR spectra (400 MHz, 298 K) of a) **1** (1 mM in $CDCl_3$/[D_6]DMSO 99:1 v/v) in the presence of D/L-tartaric acid (1.1 equiv); b) **3** (1 mM in $CDCl_3$/[D_6]DMSO 99:1 v/v) in the presence of D/L-tartaric acid (1.1 equiv); c) **1** (1 mM in $CDCl_3$/[D_6]DMSO 90:10 v/v) in the presence of D/L-tartaric acid (4 equiv); and d) **3** (1 mM in $CDCl_3$/[D_6]DMSO 90:10 v/v) in the presence of D/L-tartaric acid (4 equiv). Signals due to the empty host and the host–guest complex are marked with ○ and ●, respectively; ◆ indicate the proton resonance of the carboxylic acid of the bound guest; * indicate some signals of aromatic protons.

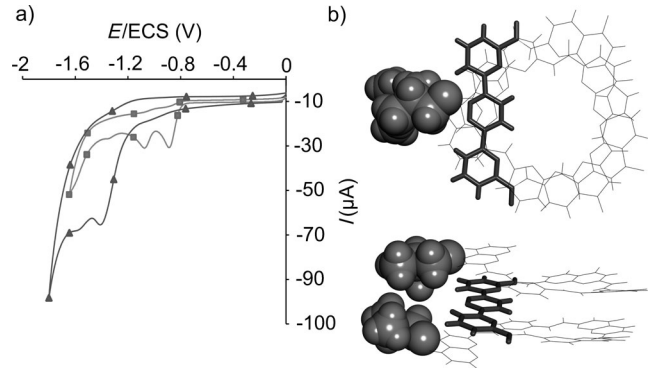

Figure 5. a) Comparison of the cyclic voltammogram of capsule **3** (▲,1 mM) and pyr-pyz-pyr **6** (■, 1 mM) at a glassy carbon electrode in THF/acetic buffer (pH 4.6)/acetonitrile (5:4:1 v/v/v) at a scan rate of 0.1 Vs^{-1}. b) Top and side view of part of the crystal structure of **1**, which shows that the pyridazine is sterically protected by two isobutoxy side chains shown as CPK. The two $\mathbf{Q_3P}$ segments at each extremity and other solubilizing side chains have been removed for clarity.

Figure 5b). In this solvent mixture, the K_a value of **3** for D/L-tartaric acid was calculated to be 1.6×10^4 $L\,mol^{-1}$, which is at least two orders of magnitude smaller than the K_a value of **1** ($>10^6$ $L\,mol^{-1}$; Table 1).

To further compare the binding properties of capsules **1** and **3** for tartaric and malic acids, a more competitive solvent mixture was used ($CDCl_3$/[D_6]DMSO 90:10 v/v) to decrease the affinities to values that can be more accurately determined by ^{1}H NMR spectroscopy titration (Table 1, see also the Supporting Information). In this solvent, the K_a values of **1** and **3** for D/L-tartaric acid were shown to be 5300 and 110 $L\,mol^{-1}$. Similarly,

Table 1. Binding constants of tartaric and malic acids to capsules **1** and **3** in solution as measured by ^{1}H NMR spectroscopy titrations at 298 K.

Entry	Guest[a]	K_a[b] [$L\,mol^{-1}$] for capsule **1**	K_a[b] [$L\,mol^{-1}$] for capsule **3**
1	D/L-tartaric acid	$>10^6$[c]	16000[c]
2	–	5300[d]	110[d]
3	D/L-malic acid	9250[c]	100[c]
4	–	70[d]	<1[d]

[a] See the Supporting Information for structures. [b] Association constant K_a measured by integration of amide peaks. [c] In $CDCl_3$/[D_6]DMSO (99:1 v/v). [d] In $CDCl_3$/[D_6]DMSO (90:10 v/v).

the affinity of **3** for malic acid was almost two orders of magnitude lower than that of **1**. Characteristic signals in the ^{1}H NMR spectra of **3**⊃D/L-tartaric acid showed that both carboxylic acid groups were hydrogen bonded to the capsule inner rim. However, their resonances were shifted upfield ($\Delta\delta\approx0.9$ ppm) from the resonances found in **1**⊃D/L-tartaric, which is consistent with the fact that **3** forms a weaker complex than **1** with tartaric acid. The ^{1}H NMR spectra of **3**⊃D/L-tartaric acid proved suitable for detailed structural studies (see the Supporting Information). The proton and carbon resonances of the helical backbone of receptor **3** encapsulating D/L-tartaric acid could be readily assigned by using 2D NMR spectroscopy with the COSY, HMQC, and HMBC techniques. Positioning of the guest in the cavity was elucidated by using ROESY which allowed us to establish several unambiguous intermolecular dipolar couplings (Figures S18 and S19 in the Supporting Information). A strong NOE contact between the C*H* of the tartaric acid and the β-pyrrolic hydrogen atoms of the central pyr-pyl-pyr segment confirmed the *anti–anti* conformation of the latter in the complex.

With the prevalence of the *anti–anti* conformation in **3**, the conversion of the pyridazine ring of **1** into the pyrrole of **3** did not result in a conformational change as dramatic as that expected for the *syn–syn* conformation. Nevertheless, even the *anti–anti* conformation of **3** proved to be sufficiently different from **1** for its guest recognition properties to be significantly diminished. As suggested by the crystal structure of **3** (Figure 3d–f) the space occupied by the pyrrolic β-protons and the change in the relative orientation of the naphthyridine units involved in direct hydrogen bonding with the guest probably explain these important differences.

In situ reduction of the capsule backbone

In addition to the stepwise synthesis of pyrrolic receptor **3**, we considered the possibility of modifying capsule backbone **2** in situ to directly obtain **3** through nitrogen extrusion of the pyridazine ring. We first attempted the preparative electrochemical reduction of **2** because the mild conditions associated with this transformation could be made compatible with guest binding by precursor **2** and thus be adjusted so that the ring contraction process would cause release of a guest molecule (Scheme 2a). As observed for isolated pyr-pyz-pyr segment **6**, used as a reference, the cyclic voltammogram of **2** showed two well-defined reduction peaks. However, the two reduction

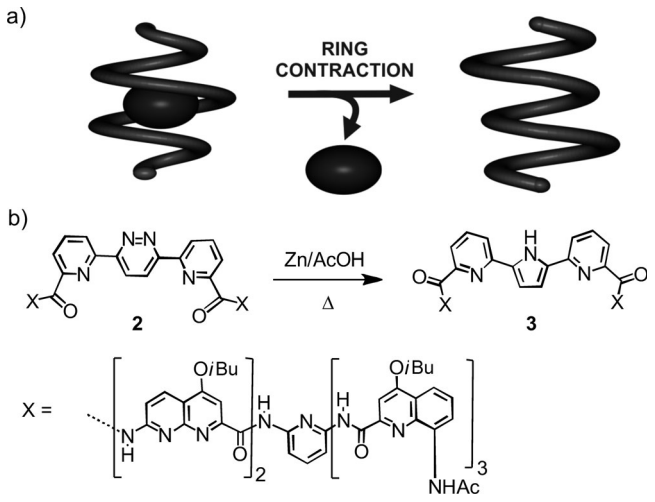

Scheme 2. a) Schematic representation of the ring-contraction-induced modification of a helix backbone that causes the release of a guest molecule. b) Reaction scheme of the direct transformation of **2** to **3**.

waves appeared at much higher cathodic potential (−1.41 and −1.57 V vs. ECS, Figure 5a), which suggests a more difficult reduction process than in **6**. A careful examination of the crystal structure of **1** revealed that two quinoline isobutoxy side chains are located above and below the pyridazine residue in the helical arrangement (Figure 5b). This positioning may act as a steric shield that could make a suitable contact between the substrate and the glassy carbon electrode difficult at the preparative level. Indeed, our attempts to carry out the electrochemical reduction of **2** remained unsuccessful.

Next, a more classical chemical reduction by using zinc in acetic acid[16] was envisaged as an alternative to the electrochemical reduction (Scheme 2b). Treating capsule **2** with zinc at reflux in glacial acetic acid afforded desired pyrrolic capsule **3** in a convincing 50% (unoptimized) yield. This result is encouraging considering the very large size of helix **2** and the location, embedded at the heart of the structure, of the selective chemical transformation that leads to pyrrolic capsule **3**. Nevertheless, glacial acetic acid at reflux is incompatible with guest binding by **2** and thus with the controlled released of a guest induced by ring contraction of a pyridazine into a pyrrole. Improvements will be required to ensure that ring contraction and host–guest chemistry occur in the same medium.

Conclusion

We have shown that the selective transformation of the structure of a single monomer at the heart of a foldamer sequence can cause a local change in helix curvature that results in significantly altered molecular recognition properties. We demonstrated that ring contraction of a pyridazine into a pyrrole within a helically folded aromatic oligoamide capsule sequence can be carried out in situ, which paves the way towards electroinduced guest release. Unexpectedly, however, an *anti–anti* conformation of the newly formed pyridyl-pyrrole-pyridyl sequence was characterized instead of the expected *syn–syn* conformation, which somewhat reduces the amplitude of the conformational change. We anticipate that oligomeric sequences comprised of several pyridazine rings that can be reduced into pyrroles may coincide to produce large-amplitude conformational changes induced by ring contraction, possibly in a cooperative manner.[8c] Future designs should also make pyridazines within the helical oligomers accessible enough to allow their electrochemical reduction under mild conditions. Research along these lines is in progress and will be reported in due course.

Experimental Section

General

All reactions were carried out under a dry nitrogen atmosphere. Commercial reagents were purchased from Sigma–Aldrich or Alfa–Aesar and were used without further purification unless otherwise specified. Chloroform and diisopropylethylamine (DIPEA) were distilled on calcium hydride (CaH_2) prior to use. Reactions were monitored by using thin layer chromatography (TLC) on Merck silica gel 60-F254 plates and observed under UV light. Chromatographic separations on silica gel were carried out by using Merck GEDURAN Si60 (40–63 μm). Proton nuclear magnetic resonance (^{1}H NMR) spectra were recorded in deuterated solvents by using 300 and 400 MHz spectrometers. Chemical shifts are reported in parts per million (ppm, δ) relative to the signal of the NMR solvent used. ^{1}H NMR splitting patterns with observed first-order coupling are designated as singlet (s), doublet (d), triplet (t). Coupling constants (J) are reported in Hz. Splitting patterns that could not be interpreted or easily visualized are designated as multiplet (m) or broad (br). ^{13}C NMR spectra were recorded at 75 or 100 MHz. Mass spectra (MS) were obtained by using matrix-assisted laser desorption/ionization (MALDI) or electrospray ionization (ESI).

Capsule 2: Diacid **5** (0.036 mmol, 0.012 g)[4c] and acetamido-hexamer amine AcNH-Q_3PN_2-NH_2 (0.072 mmol, 0.099 g)[4c] were dissolved in dry chloroform (2 mL), then DIPEA (0.18 mmol, 0.032 mL) and PyBOP (0.18 mmol, 0.094 g) were added at RT and the reaction mixture was heated to 45 °C for 12 h. The solvents were then removed under reduced pressure and the residue was purified by flash chromatography (SiO_2; eluent EtOAc/cyclohexane 20:80 v/v). The product was precipitated from a minimal amount of MeOH to give **2** as a light yellow solid (70%, 0.075 g). ^{1}H NMR (300 MHz, $CDCl_3$): δ = 11.56 (s, 2H), 11.36 (s, 2H), 10.64 (s, 2H), 9.92 (s, 2H), 9.87 (s, 2H), 8.89 (s, 2H), 8.82 (d, ^3J = 9.0 Hz, 2H), 8.68 (d, ^3J = 8.9 Hz, 2H), 8.59 (d, ^3J = 8.8 Hz, 2H), 8.45 (s, 2H), 8.37 (s, 2H), 8.27 (m, 8H), 8.18 (d, ^3J = 9.0 Hz, 2H), 7.99 (d, ^3J = 8.7 Hz, 2H), 7.87 (t, ^3J = 7.8 Hz, 2H), 7.57 (m, 6H), 7.40 (m, 8H), 7.19 (m, 4H), 6.93 (t, ^3J = 8.0 Hz, 2H), 6.72 (m, 8H), 6.3 (m, 4H), 6.01 (t, ^3J = 7.9 Hz, 2H), 4.13 (m, 8H), 3.99 (t, ^3J = 7.3 Hz, 2H), 3.86 (m, 5H), 3.72 (m, 5H), 2.82 (m, 3H), 2.36 (m, 7H), 1.28 (m, 36H), 1.10 (m, 12H), 0.57 (d, ^3J = 6.6 Hz, 6H), 0.44 ppm (d, ^3J = 6.8 Hz, 6H); ^{13}C NMR (100 MHz, $CDCl_3$): δ = 166.84; 164.04; 163.36; 163.17; 163.12; 162.95; 162.32; 161.50; 161.43; 160.46; 159.21; 154.86; 154.75; 153.69; 153.62; 153.07; 152.04; 151.54; 151.07; 150.67; 150.07; 148.93; 148.18; 148.05; 146.85; 139.69; 138.39; 137.61; 137.08; 136.50; 134.16; 134.11; 133.58; 133.13; 126.85; 126.53; 125.92; 124.57; 123.93; 123.72; 122.40; 121.59; 121.40; 116.69; 116.59; 116.22; 116.03; 115.64; 114.62; 114.44; 114.11; 113.66; 108.84; 107.74; 100.72; 98.44; 98.14; 96.94; 76.00; 75.81; 75.23; 75.16; 28.48; 28.37; 28.24; 28.15; 27.61; 23.76; 19.56; 19.53; 19.46; 19.37; 19.13; 18.47 ppm; MS (MALDI): m/z: calcd for $C_{166}H_{160}N_{34}O_{24}$ $[M+H]^+$: 3014.24; found: 3014.10.

Capsule 3: Diacid **4** (0.083 mmol, 0.026 g, see the Supporting Information) and acetamido-hexamer amine AcNH-Q_3PN_2-NH_2 (0.150 mmol, 0.202 g, see the Supporting Information) were dissolved in dry chloroform (4 mL), then DIPEA (0.30 mmol, 0.05 mL) and PyBOP (0.23 mmol, 0.120 g) were added at RT and the reaction mixture was heated at 45 °C for 24 h. The solvents were removed under reduced pressure and the residue was purified by flash chromatography (SiO_2; eluent EtOAc/dichloromethane 10:90 v/v). The product was precipitated from a minimal amount of MeOH to give **3** as a yellow solid (44%, 0.098 g). ^{1}H NMR (400 MHz, $CDCl_3$): $\delta =$ 11.73 (s, 2H), 11.53 (s, 2H), 10.69 (s, 2H), 10.56 (s, 2H), 9.78 (s, 2H), 9.38 (s, 2H), 8.89 (d, $^3J = 8.8$ Hz, 2H), 8.66 (d, $^3J = 8.8$ Hz, 2H), 8.53 (s, 2H), 8.21 (d, $^3J = 8.8$ Hz, 2H), 8.11 (m, 6H), 7.99 (d, $^3J = 7.4$ Hz, 2H), 7.91 (s, 2H), 7.62 (m, 8H), 7.49 (d, $^3J = 7.4$ Hz, 2H), 7.41 (s, 2H), 7.12 (d, $^3J = 7.7$ Hz, 2H), 6.94 (m, 10H), 6.63 (t, $^3J = 7.8$ Hz, 2H), 6.59 (d, $^3J = 8.2$ Hz, 2H), 6.16 (d, $^3J = 7.7$ Hz, 2H), 6.10 (t, $^3J = 7.8$ Hz, 2H), 6.04 (s, 2H), 5.91 (br, 1H), 4.44 (t, $^3J = 8.0$ Hz, 2H), 4.27 (m, 6H), 3.89 (t, $^3J = 6.1$ Hz, 2H), 3.74 (t, $^3J = 8.0$ Hz, 2H), 3.60 (t, $^3J = 6.6$ Hz, 2H), 3.53 (t, $^3J = 7.9$ Hz, 2H), 2.99 (m, 4H), 2.46 (m, 5H), 2.28 (m, 5H), 1.31 (m, 36H), 1.11 (m, 18H), 0.60 (d, $^3J = 6.4$ Hz, 6H), 0.13 ppm (d, $^3J = 6.5$ Hz, 6H); ^{13}C NMR (100 MHz, $CDCl_3$) $\delta =$ 166.92; 164.34; 164.13; 163.35; 163.23; 163.02; 162.96; 162.92; 161.87; 161.72; 161.31; 159.94; 154.73; 154.69; 153.89; 153.14; 153.06; 152.47; 150.63; 150.43 149.21; 148.91; 148.18; 147.45; 147.39; 138.62; 137.97; 137.76; 136.70; 136.46; 134.60; 134.01; 133.38; 133.20; 132.26; 131.56; 127.20; 126.43; 126.35; 122.84; 121.72; 121.17; 118.58; 118.15; 116.52; 116.19; 115.88; 115.69; 115.47; 115.29; 114.88; 113.79; 113.66; 112.64; 107.70; 107.50; 100.94; 98.73; 98.49; 98.37; 96.99; 76.12; 75.78; 75.28; 75.22; 75.09; 28.59; 28.45; 28.38; 28.19; 27.41; 23.90; 19.63; 19.51; 19.43; 19.37; 18.96; 18.10 ppm; MS (MALDI): *m/z*: calcd for $C_{166}H_{161}N_{34}O_{24}$ $[M+H]^+$: 3001.2435; found: 3002.5.

Crystallographic Data

See the Supporting Information. CCDC-964832 (**3**) contains the supplementary crystallographic data for this paper. These data can be obtained free of charge from The Cambridge Crystallographic Data Centre via www.ccdc.cam.ac.uk/data_request/cif.

Acknowledgements

This work was supported by an ANR grant (project no. ANR-09-BLAN-0082-01, predoctoral fellowship to C.A.) and by the Comité Interprofessionnel du Vin de Bordeaux (CIVB, predoctoral fellowship to G.L.).

Keywords: electrochemistry · foldamers · molecular capsules · molecular recognition · X-ray diffraction

[1] a) D.-W. Zhang, X. Zhao, J.-L. Hou, Z.-T. Li, *Chem. Rev.* **2012**, *112*, 5271 – 5316; b) G. Guichard, I. Huc, *Chem. Commun.* **2011**, *47*, 5933 – 5941; c) H. Juwarker, K.-S. Jeong, *Chem. Soc. Rev.* **2010**, *39*, 3664 – 3674; d) H. Juwarker, J.-M. Suk, K.-S. Jeong, *Chem. Soc. Rev.* **2009**, *38*, 3316 – 3325; e) J. Becerril, J. M. Rodriguez, I. Saraogi, A. D. Hamilton, in *Foldamers: Structure, Properties and Applications* (Eds.: S. Hecht, I. Huc), Wiley-VCH, Weinheim, **2007**, pp. 193 – 228.

[2] a) P. R. Ashton, P. J. Campbell, E. J. T. Chrystal, P. T. Glink, P. S. Menzer, D. Philip, N. Spencer, J. F. Stoddart, P. A. Tasker, D. J. Williams, *Angew. Chem.* **1995**, *107*, 1997 – 2001; *Angew. Chem. Int. Ed. Engl.* **1995**, *34*, 1865 – 1869; b) V. Berl, M. J. Krische, I. Huc, J.-M. Lehn, M. Schmutz, *Chem. Eur. J.* **2000**, *6*, 1938 – 1946; c) J.-L. Hou, X.-B. Shao, G.-J. Chen, Y.-X. Zhou, X.-K. Jiang, Z.-T. Li, *J. Am. Chem. Soc.* **2004**, *126*, 12386 – 12394; d) K.-J. Chang, B.-N. Kang, M.-H. Lee, K.-S. Jeong, *J. Am. Chem. Soc.* **2005**, *127*, 12214 – 12215; e) M. Waki, H. Abe, M. Inouye, *Angew. Chem.* **2007**, *119*, 3119 – 3121; *Angew. Chem. Int. Ed.* **2007**, *46*, 3059 – 3061; f) Y.-X. Xu, X. Zhao, X.-K. Jiang, Z.-T. Li, *J. Org. Chem.* **2009**, *74*, 7267 – 7273.

[3] a) T. Nishinaga, A. Tanatani, K. Oh, J. S. Moore, *J. Am. Chem. Soc.* **2002**, *124*, 5934 – 5935; b) A. Tanatani, T. S. Hughes, J. S. Moore, *Angew. Chem.* **2002**, *114*, 335 – 338; *Angew. Chem. Int. Ed.* **2002**, *41*, 325 – 328; c) Q. Gan, Y. Ferrand, C. Bao, B. Kauffmann, A. Grélard, H. Jiang, I. Huc, *Science* **2011**, *331*, 1172 – 1175; d) Y. Ferrand, Q. Gan, B. Kauffmann, H. Jiang, I. Huc, *Angew. Chem.* **2011**, *123*, 7714 – 7717; *Angew. Chem. Int. Ed.* **2011**, *50*, 7572 – 7575; e) Q. Gan, Y. Ferrand, N. Chandramouli, B. Kauffmann, C. Aube, D. Dubreuil, I. Huc, *J. Am. Chem. Soc.* **2012**, *134*, 15656 – 15659.

[4] a) J. Garric, J.-M. Léger, I. Huc, *Angew. Chem.* **2005**, *117*, 1990 – 1994; *Angew. Chem. Int. Ed.* **2005**, *44*, 1954 – 1958; b) C. Bao, B. Kauffmann, Q. Gan, K. Srinivas, H. Jiang, I. Huc, *Angew. Chem.* **2008**, *120*, 4221; *Angew. Chem. Int. Ed.* **2008**, *47*, 4153; c) Y. Ferrand, A. M. Kendhale, B. Kauffmann, A. Grélard, C. Marie, V. Blot, M. Pipelier, D. Dubreuil, I. Huc, *J. Am. Chem. Soc.* **2010**, *132*, 7858 – 7859.

[5] C. Bao, Q. Gan, B. Kauffmann, H. Jiang, I. Huc, *Chem. Eur. J.* **2009**, *15*, 11530 – 11536.

[6] Y. Ferrand, N. Chandramouli, A. M. Kendhale, C. Aube, B. Kauffmann, A. Grélard, M. Laguerre, D. Dubreuil, I. Huc, *J. Am. Chem. Soc.* **2012**, *134*, 11282 – 11288.

[7] a) E. Aznar, M. D. Marcos, R. Martinez-Manez, F. Sancenon, J. Soto, P. Amoros, C. Guillem, *J. Am. Chem. Soc.* **2009**, *131*, 6833 – 6843; b) P. K. Lo, P. Karam, F. A. Aldaye, C. K. McLaughlin, G. D. Hamblin, G. Cosa, H. F. Sleiman, *Nat. Chem.* **2010**, *2*, 319 – 328; c) J. W. Brown, B. L. Henderson, M. D. Kiesz, A. C. Whalley, W. Morris, S. Grunder, H. Deng, H. Furukawa, J. I. Zink, J. F. Stoddart, O. M. Yaghi, *Chem. Sci.* **2013**, *4*, 2858 – 2864; d) M. Han, R. Michel, B. He, Y.-S. Chen, D. Stalke, M. John, G. H. Clever, *Angew. Chem.* **2013**, *125*, 1358 – 1362; *Angew. Chem. Int. Ed.* **2013**, *52*, 1319 – 1323.

[8] a) C. Tie, J. C. Gallucci, J. R. Parquette, *J. Am. Chem. Soc.* **2006**, *128*, 1162 – 1171; b) Z. Yu, S. Hecht, *Angew. Chem.* **2011**, *123*, 1678 – 1681; *Angew. Chem. Int. Ed.* **2011**, *50*, 1640 – 1643; c) Z. Yu, S. Hecht, *Chem. Eur. J.* **2012**, *18*, 10519 – 10524.

[9] a) R. B. Prince, T. Okada, J. S. Moore, *Angew. Chem.* **1999**, *111*, 245 – 249; *Angew. Chem. Int. Ed.* **1999**, *38*, 233 – 236; b) M. Barboiu, J.-M. Lehn, *Proc. Natl. Acad. Sci. USA* **2002**, *99*, 5201 – 5206; c) A.-M. Stadler, N. Kyritsakas, J.-M. Lehn, *Chem. Commun.* **2004**, 2024 – 2025; d) H. Juwarker, J. M. Lenhardt, D. M. Pham, S. L. Craig, *Angew. Chem.* **2008**, *120*, 3800 – 3803; *Angew. Chem. Int. Ed.* **2008**, *47*, 3740 – 3743.

[10] a) C. Dolain, V. Maurizot, I. Huc, *Angew. Chem.* **2003**, *115*, 2844 – 2846; *Angew. Chem. Int. Ed.* **2003**, *42*, 2738 – 2740; b) E. Kolomiets, V. Berl, I. Odriozola, A.-M. Stadler, N. Kyritsakas, J.-M. Lehn, *Chem. Commun.* **2003**, 2868 – 2869; c) I. Okamoto, M. Nabeta, Y. Hayakawa, N. Morita, T. Takeya, H. Masu, I. Azumaya, O. Tamura, *J. Am. Chem. Soc.* **2007**, *129*, 1892 – 1893.

[11] a) Y. Hua, A. H. Flood, *J. Am. Chem. Soc.* **2010**, *132*, 12838 – 12840; b) Y. Wang, F. Bie, H. Jiang, *Org. Lett.* **2010**, *12*, 3630 – 3633.

[12] a) H. Bakkali, C. Marie, A. Ly, C. Thobie-Gautier, J. Graton, M. Pipelier, S. Sengmany, E. Léonel, J. Y. Nédélec, M. Evain, D. Dubreuil, *Eur. J. Org. Chem.* **2008**, 2156 – 2166; b) S. Naud, M. Pipelier, G. Viault, A. Adjou, F. Huet, S. Legoupy, A. M. Aubertin, M. Evain, D. Dubreuil, *Eur. J. Org. Chem.* **2007**, 3296 – 3310.

[13] A. Tabatchnik-Rebillon, C. Aubé, H. Bakkali, T. Delaunay, G. T. Manh, V. Blot, C. Thobie-Gautier, E. Renault, A. Planchat, J.-Y. Le Questel, B. Kauffmann, Y. Ferrand, I. Huc, K. Urgin, S. Condon, E. Léonel, M. Evain, J. Lebreton, D. Jacquemin, M. Pipelier, D. Dubreuil, *Chem. Eur. J.* **2010**, *16*, 11876 – 11889.

[14] T. Qi, T. Deschrijver, I. Huc, *Nat. Protoc.* **2013**, *8*, 693 – 708.

[15] R. A. Laskowski, *J. Mol. Graphics* **1995**, *13*, 323 – 330.

[16] a) D. L. Boger, C. E. Brotherton-Pleiss, *Advances in Cycloaddition, Vol. 2* (Ed.: D. P. Curran), Jai, Greenwitch, **1990**; b) D. L. Boger, *Tetrahedron* **1983**, *39*, 2869 – 2939.

Received: October 7, 2013
Published online on January 8, 2014